

# Estimation of Formation Pressure by using a New approach Along with Other Techniques in Two Selected Wells in Rumaila and Zubair fields

Sarah Thayer Haider<sup>1</sup>, Dr. Rafid Kadhim Abbas<sup>2</sup>, Dr. Aqeel Al-Adili<sup>3</sup>

<sup>1</sup>University of Technology, Petroleum Technology Dept. Baghdad, Iraq  
sarhtha1994@gmail.com

<sup>2</sup>University of AL-Qadisiyah, Faculty of Engineering, Dept. of Chemical Engineering, AL-Diwaniyah, Iraq  
Rafid.Abbas@qu.edu.iq

<sup>3</sup>University of Technology, Applied Science Dept. Baghdad, Iraq  
aqeel@uotechnology

## Article Info

Volume 83

Page Number: 10373 - 10391

Publication Issue:

March - April 2020

## Abstract:

Many studies indicated that the abnormal pore pressure (overpressure) could be a dilemma when drilling wells due to the severe effects might occur that raise the cost to unbelievable rates. If overpressure happened, this could lead to several problems for instance kick, blowout and also to a geological disaster such as volcano eruption through the drilling, therefore the anticipation of this pressure is vital to prevent drilling problems.

The objective of this study is the real-time predication of pore pressure of two selected oil producing wells in Rumaila and Zubair fields in south Iraq region. Various approaches are used for this purpose such as the modified specific energy along with Rabia's formula of specific energy as well as from well logs. The calculated pore pressures are compared with the actual formation pressure obtained from Real Formation Test (RFT) and Measurements While Drilling (MWD) logs. The statistical comparison according the Mean Absolute Error (MAE) showed that the new suggested formula of pore pressure determination is the best among the other techniques being used in the present study leading to the possibility to apply the new technique on other wells in the same area and might on other regions.

**Keywords:** pore pressure, formation pressure, specific energy, well logs

## Article History

Article Received: 24 July 2019

Revised: 12 September 2019

Accepted: 15 February 2020

Publication: 13 April 2020

## I. Introduction

Pore pressure or also called formation pressure defined as the pressure exerted by the fluid within the pore spaces of the rock. Pore pressure is classified into three categories: hydrostatic pore pressure, overpressure or abnormal and subnormal pore pressure. When pore pressure is greater than normal pore pressure, it is named as abnormal formation pressure. (Jincai Zhang 20117)

Nowadays, the most significant target of any drilling operation is reducing the cost and also to avoid drilling issues or minimizing the hazards of

drilling problems which may happen like, blowouts, kick, stuck pipes, loss circulation, lost hole, and casing setting issues. (Jincai Zhang 2017) Abnormal pressure is considered one of the issues that cause severe drilling dilemmas; therefore, predicting the pore pressure during drilling is significant in order to use the suitable drilling mud to control the well.

Abnormal formation pressure is occurred in many formations around the world due to various causes mainly referred to geological effects that gives an

indication that the issue should be handled as otherwise, severe dilemmas could appear.

South Iraq region is influenced by a geological thrust and the occurrence of salt series at deep depths that lead to make south Iraq region exposed to be a place for occurring overpressure (Abbas, 1996).

South Rumaila field is situated in southern Iraq, near Basra district and about 32 km (20 mile) from the Kuwaiti border. South Rumaila field is a super-giant oil field that considered the third biggest oilfield in the world (Abd Al-Razzaq *et al*., 2016) and (Al-Hameedi *et al.*, 2017).

There are three types of pore pressure including the following: 1-Normal pore pressure where the pore pressure gradient is very close to the hydrostatic formation pressure gradient, 2- Abnormal pore pressure where the pore pressure gradient is greater or lesser than the normal pore pressure gradient. If it is abnormally high, the pressure is called overpressure or abnormally low or subnormal where it is called surpressure.

Pore pressure gradient is depending on many factors such as:(temperature, concentration of dissolved salt in formation water, pore fluid sort) as illustrated by Swarbrick and Osborne, (1998).

Abbas (1996) achieved a study about how we can predict and calculate the abnormal pressure in some selected wells in southern Iraq. Abbas (1996) used various detection strategies to anticipate the overpressure zones and also the research showed that the formation pressure was obtained from different techniques. The study depended on using the data collected from mud and sonic logs. In this study overpressure occurred in three deep formations: Yamama, Sulaiy and Gotnia. It was illustrated that the main reason causing abnormal formation pressure (overpressure) in southern Iraq is salt series through Gotnia formation. Estimation of pore pressure as well as abnormal formation pressure zones has been performed by means of: d-exponent, dc – exponent, sigma log, ROP, flow line temperature, delta temperature, total gas, association gas, and sonic log.

Morteza Azadpour and Navid Shad Manaman (2015) studied the prediction of abnormal pressure in south Iran carbonate reservoir rocks. The purpose from this study was to assess pore

pressure within carbonate reservoirs by applying Weakley's approach and comparing the results with pore pressure predicted from Eaton's method. They used different strategies of detection of overpressure in southern Iran. The forecasting of overpressure based on well logs data (sonic log, gamma ray and density log) where two methods were applied (Eaton's method with some modifications and Weakley's approach). In this study, abnormal pressure occurred in five formations: Asmari, Pabdeh, Gurpi, Ilam, and Sarvak.

Al-Hameed, A.T., Dunn-Norman, et (2017) made a study about how we can prediction mud loss circulation in south of Iraq. this study occurred in Rumelia field in Dammam formation because loss circulation is a big problem in Damam formation (75 wells). so the aim of this study to predication the best values of drilling parameters because mud losses is depended on Drilling parameters in this formation. so they used Detection strategies show that loss circulation in south of Iraq .so Estimation of loss circulation has been reached by three ways: Rop(rate of penetration) ,MW(mud weight), ECD ( equivalent circulated density ) . they concluded the three ways used in this study can be used to predication excepted of the Mud losses in Dammam formation.

Chen Xin et al. (2016) carried out a study about pore pressure prediction relied on seismic data in south west of Iraq. Overpressure in southwest Iraq was predicted by three methods: 1- Using under-compaction theory, using Eaton method and Equivalent depth, 2- Logging data, using Bowers and Philips methods, 3- Seismic data. Depending on Fillipone formula & modified Fillipone formula. In this study, the results showed that the predication of pore pressure was close to actual pore pressure. The error percent was less than 5% according to measured data by drilling test. This method is considered a good approach for pore pressure predication before drilling (Chen Xin *et al.*, 2016).

Marcia *et al.* (2018) suggested new monitoring and control strategies to manage pressure fluctuations during oil well drilling. The purpose of this study was to control real-time downhole pressures that could be exposed to disturbances. Experimental and simulation processes were

carried out to avoid kick and mud losses resulted from abnormal pore pressure.

**Olalere and Buttb (2019)** performed a research on the possibility of abnormal pressure predication depending on drilling parameters using the concept of Specific Mechanical Energy (MES) and Hydro- Mechanical Energy (HMSE). The authors elucidated the possibility of abnormal pressure predication from MES and HMSE in Niger Delta basin. They showed that the main reason causes abnormal pressure is under compaction in this area. The obtained results illustrated that the predicated pore pressure depended on specific energy is close to actual pore pressure. In addition, this approach pore pressure could be calculated from drilling parameters in case of no available downhole measurements.

## 2. Theoretical Background

Generally, many techniques are used for pore pressure determination in oil wells. Three main formulas showed by (Eaton, 1972) and (Eaton, 1975) are presently useful to compute the formation pore pressure. The proposed equations for the determination of pore pressure are displayed as follows:

$$G_{pp} = G_{ob} - \{ G_{ob} - G_{np} \} \left[ \frac{\Delta t_n}{\Delta t} \right]^3 \dots\dots(1)$$

$$G_{pp} = G_{ob} - \{ G_{ob} - G_{np} \} \left[ \frac{RO}{Rn} \right]^{1.2} \dots\dots (2)$$

$$G_{pp} = G_{ob} - \{ G_{ob} - G_{np} \} \left[ \frac{dco}{dcn} \right]^{1.2} \dots\dots(3)$$

where,  $G_{pp}$ ,  $G_{ob}$  and  $G_{np}$  are predicted pore pressure gradient, overburden pressure gradient and normal pressure gradient respectively (psi/ft).

Abnormal pore pressure estimation might be achieved by modifying the specific energy formula which is based on the idea that overpressure intervals that have low effective stress need less energy to excavate than the intervals that have hydrostatic pressure at an equivalent depth. In the present study, Eaton's formula for determining pore pressure is modified depending on the conception of specific energy as follows:

$$G_{pp} = G_{ob} - (G_{ob} - G_{np})^m \left[ \frac{SE_o}{SE_n} \right] \dots\dots\dots (4)$$

Where,  $SE_o$  is the observed specific energy (psi),  $SE_n$  is the specific energy from the normal trend line (psi) and  $m$  is an exponent should be accordingly determined. The exponent ( $m$ ) could be estimated from the following equations:

$$G_{ob} - G_{pp} = \frac{SE_o}{SE_n} \{ G_{ob} - G_{np} \}^m \left[ \frac{SE_o}{SE_n} \right] \dots\dots\dots (5)$$

$$\log(G_{ob} - G_{pp}) = \log(G_{ob} - G_{np}) + m \log \left[ \frac{SE_o}{SE_n} \right] \dots\dots\dots(6)$$

$$\frac{\log(G_{ob} - G_{pp})}{\log(G_{ob} - G_{np})} = m \log \left[ \frac{SE_o}{SE_n} \right] \dots\dots\dots (7)$$

Plotting  $\log [(G_{ob}-G_{pp})/(G_{ob}-G_{np})]$  vs.  $\log [SE_o/SE_n]$ , the slope ( $m$ ) could be determined. The normal compaction trend line must be recognized; where the values of the plot are increased linearly without anomalies as such values are found in clean shale formations. At normal pressure zones, the values of SE will rise with depth, whereas at high abnormal pressure intervals, the values of SE will be decreased. Equation (4) is used to determine the formation pore pressure, where the specific energy should be determined firstly.

A modified specific energy formula was postulated by (Abbas, 2017) depending only on two factors 1-Hardness of the drill bit 2-Hardness of the rock formations being drilled as follows:

$$SE_o = \frac{28137.862 H_w}{(H_w/H_a)^{2.5}} \dots\dots\dots (8)$$

where  $H_a$  is the hardness of the bit ( $N/m^2$ ),  $H_w$  is hardness of the rock being excavated ( $N/m^2$ ) and  $SE_o$  is the observed specific energy (psi).

In the literature, when torque values are not measured, the recommended formula of specific energy determination is found by **Rabia (1985)** as follows.

$$SE = 20 \frac{W \cdot N}{d \cdot ROP} \dots\dots\dots(9)$$

where,  $W$  is the weight on bit (lb),  $d$  is the diameter of the bit (in),  $N$  is the speed rotation (RPM), and  $ROP$  is the penetration rate (ft./hr) and  $SE$  in  $lb/in^2$  (psi). The aforementioned formula of the specific energy could be implemented when torque is unavailable within the bit record data.

The specific energy values obtained by the two aforementioned formulas in equation (8) and (9) are used to compute the formation pore pressure from equation (4). In addition, pore pressure is predicted by Eaton's method (equation 1). All techniques used in the present study for pore pressure estimation are compared with the actual pore pressure obtained from Repeated Flow Test (RFT) and from the Measurements While Drilling logs (MWD). A statistical analysis must be taken into account to assess the results being obtained from the new modified formula of pore pressure (equation 4). Mean Absolute Error (MAE) is calculated from equation (10) (Peter, 1964).

$$MAE = \left[ \frac{1}{N} \sum_{i=1}^n \left| \frac{A(I)_m - A(I)_c}{A(I)_m} \right| \right] \dots (10)$$

where,  $MAE$  is dimensionless (%),  $A(I)_m$  is the measured (actual) values of pore pressure measured from RFT and MWD logs,  $A(I)_c$  is the calculated values of pore pressure from specific energy approach, and  $n$  is the number of readings. This statistical method could verify the approaches used to estimate the pore pressure by comparing the calculated values for any model with the actual values, where the model that has the lowest value of  $MAE$  is the most nearest to the actual.

### 3-Collection of data

The essential data used for the calculations in the present study are collected from the final bit records, well logs (density, sonic and resistivity) as well as from the geological reports of Rumelia and Zubair fields in south of Iraq provided by the Ministry of oil in Iraq, Baghdad. In this research, two selected wells are chosen one in Rumaila field (Ru-131), whereas the other is in Zubair field (Zu-42).

The actual pore pressure is taken from RFT and MWD logs provided from the Ministry of oil in Iraq. Data of tables (1) and (2) are quoted from drilling report and geological final report provided from the Ministry of oil.

### 4-Results and discussion

#### For Ru-131

The  $SE$  (Specific Energy) values obtained from the new modified formula (Equation-8) are plotted versus depth as displayed in fig (1). The resulted values of  $SE$  are displayed in the first columns in table (2).

In this well, the specific energy is affected by two main parameters; the hardness of the rock formation as well as the hardness of the materials that forming the bit that excavates the well as clearly seen in equation (8). The normal compaction trend line (NTC) is drawn for the values of  $SE$  been increasing gradually and usually in clean shale formations. In this formation the amount of rock compaction is increased leads to reduce pore pressure and increase specific energy that is required to remove unit volume of rock. Fig (2) shows the log-log plot to determine the value of the exponent ( $m$ ) in Equation (4). Fig (2) illustrates that the value of ( $m$ ) for well Ru-131 was (0.0911), while fig. (3) displays the plot of the pore pressure predicted from the new suggested formula in equation (4) with the actual pore pressure versus depth. The calculations are demonstrated in the two last columns in table (2). The actual pore pressure measurements were taken from MWD and RFT logs. As seen from fig. (3), the predicted results of formation pressure show a good rapprochement with the actual pore pressure. From the surface until nearly depth (2100 m), the predicted pore pressure from the new model is very close to the actual formation pressure until depth 2100 m. When depth reaches (2100 m) until depth (2198 m) which is corresponded to Tanuma and Khasib formations respectively, the anticipated pore pressure is slightly higher than the hydrostatic pore pressure, which gives an indication that at these formations a very slight overpressure might occur near (2100-2198 m) depth in north Rumaila field. This slight increase in pore pressure is attributed to the occurrence of shale formation where such formations show low permeability

which yielded to under-compaction phenomena that happens in rapidly subsiding basins (Almalikee and Al-Najim, 2018). Further down at approximately depth (2200 m) to (2370 m), the forecasted The corresponded formation at this depth is Mishrif reservoir formation. The predicated formation pore pressure at this formation is decreased to values lower than the hydrostatic pore pressure due to hydrocarbon production at Mishrif formation. At Rumaila formation about (2374 m) depth, the predicated formation pore pressure is returned to values near the hydrostatic pore pressure and this scenario is extended until depth near (3100 m) which represents upper Zubair formation where consider as main oil producing reservoir causing the predicted pore pressure to be lower than the hydrostatic pressure due to hydrocarbon production at this formation a long time ago causing pore pressure to be dropped. The drop in pore pressure extended to depth (3375 m), where the predicted pore pressure is back again to a trend near the hydrostatic pressure near Zubair (sandstone) formation. At near depth (3448 m) that corresponded to Ratawi formation, the forecasted pore pressure is started to increase to a trend higher than the hydrostatic pressure.. When the depth is deeper to almost (3500 m) Yamama formation is encountered where, the predicted pore pressure gradient escalated to a about 0.52 psi/ft until reaching depth of (3775 m) , the indication of entering an abnormal pressure zone is appeared as estimated the formation pressure from the new model increased dramatically from 0.52 psi/ft to 0.654 psi/ft. Yamama formation as shown in the previous studies is an overpressure zone (Abbas, 1996). Going beyond depth (3900 m), Sulaiy formation is being entered , where also the predicted as well as the actual pore pressure gradient is still above the hydrostatic gradient which considered an abnormal pressure zone.

It is worth mentioning that, the predicted pore pressure from the new model when compared with the actual pore pressure as shown in fig. (3), the predicted pressure gradient from depth (3050 m) until depth (3350 m) is slightly more than the actual pressure gradient, but the two pressure returned to be very close until depth (3450 m) , the actual gradient is being slightly higher than the

predicted gradient till the end except at some depths.

The plot of *SE* (Specific Energy) obtained from the Rabia's formula versus depth is displayed in fig. (4) *SE* values are computed from equation (9) and the results are shown in table (3). The drilling information being used in the calculation of the specific energy from this approach includes weight of bit, rate of penetration (*ROP*), speed rotation and diameter of the bit. The specific energy is affected by these parameters, so when the speed of bit is reduced, *ROP* increases with decrease in specific energy values leading to an increase in pore pressure formations. The normal compaction trend line (NTC) is drawn for the values of *SE* been increasing gradually which is attributed to the occurrence of subsurface overpressure conditions. In such formations the amount of rock compaction is increased leads to a reduction in pore pressure and increase in specific energy values that is required to remove unit volume of rock. Fig. (5) shows the determination of the exponent (*m*) in equation (4) from Rabia's formula. Fig. (5) illustrates that the produced value of (*m*) was 0.1419, while fig. (6) displays the plot of the pore pressure gradient resulted from the new suggested formula based on the specific energy calculated from Rabia along with the actual pore pressure gradient versus depth. The calculation results are demonstrated in table (3). The actual pore pressure measurements were taken from MWD and RFT logs. At depth ranges (493-944 m), the predicated pore pressure gradient with the actual one is slightly increased via formations of (Fars, Dammam and Ghar). At depth ranges (945-1537 m), the forecasted formation pressure matches exactly the actual pore pressure passing formations of (Rus and Umm Er Redhuma). At depth ranges (2000-3400 m) , the predicated pore pressure gradient exhibits the same trend of the actual pore pressure , but slightly higher than it. Beyond depth of (3400 m) till the end near (4000 m), the predicted pore pressure gradients as well as the actual one display overpressure as the formations passed are indicated in the literature as abnormal pressure zones especially, Yamama and Sulaiy). As an overall, the predicted pressure gradient from the new method that uses Rabia's equation of specific

energy shows a good agreement with the actual pressure gradient.

The formation pressure is also determined from sonic logs using Eaton formula (Equation 1). Plotting the transit time vs. depth as the normal compaction trend line (NTC) is shown in fig. (7) represents the normal hydrostatic pressure. The results of the estimated pore pressure are illustrated in table (4). Fig. (8) displays the plot of the pore pressure predicated resulted from Eaton's formula with the actual pore pressure versus depth . At depth ranges (2000-2200 m) , the predicated pore pressure increases with depth entering the formations called (Sadi , Tanuma and Khasib), as these formations contain high parentage of shale , especially at Tanuma formation and these shale layers have low permeability due to the phenomenon of under-compaction. when reaching depth near (2200 m) passing through Mishrif formation , the forecasted pore pressure decreases sharply because the pore pressure predicated is lower than hydrostatic pore pressure due to hydrocarbons production in this formation. At depth ranges (2375-3000 m), the predicated pore pressure gradient is fluctuated near the actual pore pressure gradient. At depth ranges (3000-3100 m), the predicted pressure gradient is decreased in a trend lower than the usual trend leading to a zone of surpressure through the first part of Zubair formation which considered as an oil production zone.

#### For Zb- 42

The same previous aforementioned calculations were performed again on well Zu-42. Figures (9, 10) show the specific energy determined vs. depth and the determination of the slope  $m$  which was equal to 0.1796. Fig. (11) displays the plot of the pore pressure gradient resulted from the new suggested formula with the actual pore pressure versus depth. It is worth mentioning, that fig. (11) shows clearly a very good agreement between the predicted and the actual pressure gradient. Similar to the obtained aforementioned results from well

Ru-131, the overpressure and surpressure zones are shown, but the difference they are occurred at slight different depths. Figures (12,13) show the specific energy obtained from Rabia's approach vs. depth and the determination of the slope  $m$  respectively. At depth ranges (3005 -3395 m) as shown in fig. (14) , the estimated pore pressure gradient is close to the actual gradient ,but at some depths the predicted pore pressure seems to be fluctuated around the actual pressure.

The normal compaction trend lines (NTC) are drawn for the values of ( $\Delta t_n$ ) derived from sonic log as shown in fig. (15). Fig. (16) displays the plot of the predicated pore pressure gradient resulted from equation (1) with the actual pore pressure gradient versus depth . It is worth mentioning that, from depth (2380 m) to (3650 m) the forecasted pore pressure is close to the actual pore pressure, but afterwards, the predicted formation pressure from Eaton method is showing a divergence with the actual pressure except at depth ranges (3948-3975 m).

For a better understanding of the closest approach being used with the actual pore pressure, *MAE* is used for the statistical analysis. *MAE* is calculated from equation (10). This equation is used to compare the measured values with the calculated ones for any model. Therefore, the model that has the lowest *MAE* is considered the best among the models.

Results of *MAE* for well Ru-131 are **(18.32%,11.89%,42.11%)** for the new model based on Abbas' equation, new model based on Rabia's formula and from Eaton (sonic log) respectively.

On the other hand, for well Zb-42, *MAE* values are **(11.54%,15.64,18.43%)** for the suggested model using Abbas' equation, new model relied on Rabia's formula and from Eaton's equation respectively.

Fig.(17,18) demonstrates the histogram of *MAE* values for wells Ru-131 and Zu-42. The results obtained from *MAE* displayed that the new approach for pore pressure determination is considered a good and reliable as it has very low *MAE* compared with other methods. In contrast, pore pressure gradient determined by sonic log is the worst according to *MAE*, therefore, the pore pressure gradient predicated by the new suggested model in this research is considered a good approach to predict pore pressure in case of the unavailability of well logs

### 5-Conclusions

- 1-The new suggested model based on specific energy technique is concluded to be a good and acceptable approach to estimate pore pressure gradient especially, when well logs are unavailable.
- 2- From the obtained results, the new approach was found to be closest to the actual pore pressure

as the value of *MAE* was the lowest compared to other techniques being used in the present work.

3- It is possible to calculate the *SE* values from other approaches such as Teale's equations, but this option is limited on the availability of the torque. As torque is not always available and also the techniques that measure the real-time torque is not precise, therefore well logs with special tools are used for this purpose.

### Acknowledgments

Herein, I must express my deep gratitude to the Ministry of oil in Iraq for providing the indispensable data used in this research. Thanks are extended to my supervisors who supported and provided me with valuable advice throughout the work.

Table 1. Sample of data obtained from bit record, well logs and geological information for Ru -131

Depth (m)	Gob (psi/ft)	Gpp (psi/ft)	Bit commercia	Bit type	H <sub>a</sub> of bit	H <sub>w</sub> of rock	Formation
100	0.78002	0.4696	k2	Milled-tooth	12.95		Dibdibaa
200	0.78002	0.467	k2	Milled-tooth	12.95		Dibdibaa
300	0.8233545	0.4695	k2	Milled-tooth	12.95		Dibdibaa
400	0.8233545	0.46876	k2	Milled-tooth	12.95		Dibdibaa
500	0.8666889	0.4696	M-J	Milled-tooth	12.95		Lower Fars
600	0.9100234	0.46686	M-J	Milled-tooth	12.95		Ghar
2425	1.0790277	0.468	SVH	Milled-tooth	12.95		Rumaila
2450	1.0573605	0.469512195	SVH	Milled-tooth	12.95		Rumaila
2500	1.014026	0.469512195	SVH	Milled-tooth	12.95		Ahmadi
2550	1.0573605	0.469512195	SVH	Milled-tooth	12.95		Ahmadi

3100	1.0313598	0.344217152	J33	Insert tooth	15	Shuaiba
3150	1.0183595	0.342624855	J33	Insert tooth	15	Zubiar
3300	1.0096926	0.303030303	C22	Milled-tooth	12.95	Zubiar
3350	0.9533578	0.414	C22	Milled-tooth	12.95	Zubiar
3675	1.1664663	0.622383684	M88	insert tooth	15	Yamama
3700	1.1207841	0.62301	J33	insert tooth	15	Yamama
3900	1.1257688	0.618	J33	insert tooth	15	Yamama
3925	1.1468064	0.625	J33	insert tooth	15	Yamama
3950	1.1337096	0.63235	J33	insert tooth	15	Yamama
3973	1.159606	0.6389	J33	insert tooth	15	Sulaiy

Table 2. Results of Ru-131 by implementing the new suggested formula of pore pressure

Depth (m)	SE observed (Mpsi)	SE normal (Mpsi)	Actual Gpp (psi/ft)	Predicted Gpp (psi/ft)
100	194528.8866	213818	0.469512195	0.474641586
200	193174.1888	216000	0.467	0.475118092
300	192724.1243	216000	0.4695	0.475630665
2400	242624.9536	264000	0.469507114	0.476053539
2425	252301.1472	264000	0.468	0.474501354
2450	242624.9536	261818	0.469511	0.476045835
2500	286549.1736	264000	0.469545	0.467937733
2550	235803.5367	261000	0.46901	0.477388808
2600	246945.8029	261000	0.46602	0.47503145
2650	262610.9348	261000	0.469512195	0.471696079
2675	252157.5751	261818	0.469512195	0.473734701
2700	253632.3823	264000	0.46944	0.474369338
2750	247866.8128	266181	0.46951	0.475929303
2800	215921.5523	266181	0.46865	0.481335038
3100	365379.2939	277090	0.344217152	0.457726355
3150	358331.2534	277090	0.342624855	0.459051445
3200	302814.3122	277090	0.341082317	0.4683375
3250	337951.1466	277090	0.3212	0.464083721
3300	518963.7605	279272	0.303030303	0.440774243
3350	458102.2779	279272	0.414	0.449800846
3375	403813.3215	279272	0.469512195	0.454665946
3380	401529.7457	279272	0.47166	0.453042347
3390	311147.4445	279272	0.447	0.466207985

3400	337218.2045	281454	0.4823	0.463791836
3425	357768.6504	281454	0.495	0.458777968
3450	187955.1966	283636	0.509	0.490188743
3475	177015.1522	283636	0.517	0.487864163
3605	71901.24652	285818	0.62063	0.546401826
3625	90858.48069	285818	0.6211	0.537333814
3650	59357.73391	2901881	0.621757368	0.669481494
3675	46819.81605	2901881	0.622383684	0.68962131
3700	45362.66162	2901881	0.62301	0.676587419
3725	46525.74901	2901881	0.63263	0.666632255
3750	62923.33662	2901881	0.6242	0.645442321
3775	59357.73391	2901881	0.625	0.654804252
3800	46819.81605	292363	0.6255	0.561884734
3825	45362.66162	292363	0.626	0.563212986
3850	46525.74901	292363	0.62614	0.577004782
3875	62923.33662	292363	0.62739	0.552947591
3900	59357.73391	292363	0.618	0.560386196
3925	46819.81605	292363	0.625	0.575709489
3950	45362.66162	292363	0.63235	0.575307375
3973	46525.74901	292363	0.6389	0.578010556

Table 3. Sample of results by obtained from the new model of pore pressure gradient prediction using Rabia's results of specific energy

Depth (m)	SE ,from Rabia, (psi)	SEn, ( psi)	Predicted Gpp (psi/ft)	Actual Gpp (psi/ft)
493	91093.34791	31347	0.407495261	0.469512195
735	143980.1883	68965	0.423774033	0.469512195
944	118958.6656	100313	0.460319483	0.469512195
1537	222635.2105	181818	0.455754631	0.469512195
1664	467154.0017	200626	0.400999702	0.469512195
2004	518523.7038	244514	0.397328646	0.458874933
2020	351299.8093	257053	0.442132457	0.463233518
2227	356768.796	282131	0.451148194	0.340083948
2630	274688.7037	344827	0.494027366	0.469512195
3060	585600.0937	401253	0.444517341	0.393352463
3270	405820.8649	445141	0.476863112	0.314201537
3286.5	1667807.818	445141	0.361155586	0.30803212
3316.9	520356.0392	445141	0.461314199	0.34120133
3505	860832.1377	470219	0.436637415	0.6181
3611	244554.5846	489028	0.518704411	0.6207
3612	135868.2832	489028	0.559192662	0.6208
3632	145412.6402	952297	0.612062158	0.6213
3667	162805.1324	952297	0.620027152	0.6221

3682	146697.2041	952297	0.618561317	0.6225
3700	190437.1962	501567	0.554946356	0.62302
3811.1	261102.5709	514106	0.522080809	0.6258
3898.5	198743.4994	526645	0.554873642	0.62798
3972.4	220435.2678	532515	0.55615644	0.63878

Table. (4).Sample of predicted pore pressure gradient results obtained from Eaton method for Ru-131

Depth (m)	Normal travel time (µsec/ft)	Predicted Gpp from Eaton method (psi/ft)	Actual Gpp (psi/ft)
1899.75	77.98	0.695640016	0.457154985
1900	76.64	0.696246462	0.457156611
<b>2000</b>	72.15	0.18360035	0.45777439
2375	67.22	0.495655825	0.469507114
2400	67.66	0.683588558	0.469512195
2450	66.35	0.888362197	0.469512195
2500	63.95	0.513177906	0.469512195
2600	62.15	0.745365623	0.469512195
2700	60	0.457014265	0.469512195
2800	59.87	0.884583633	0.469512195
2900	58.67	0.859875784	0.469512195
3000	55.33	0.661715208	0.344217152
3100	58.93	0.831715599	0.341082317
3200	57.2	0.858701864	0.303030303
3300	53.3	0.792151421	0.469467028

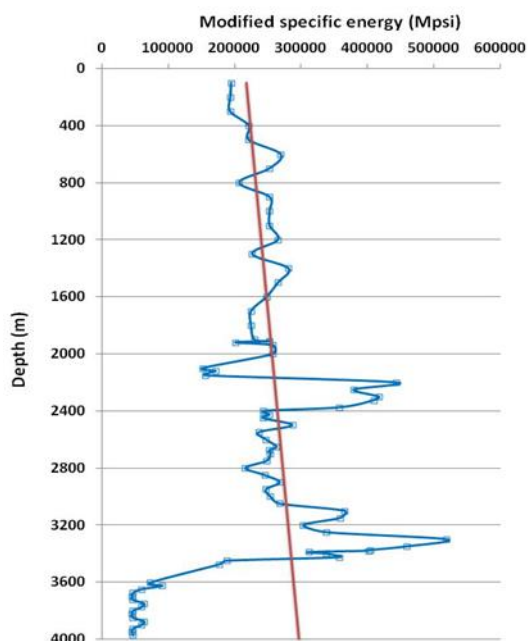


Figure (1) Specific energy obtained from modified new formula versus depth

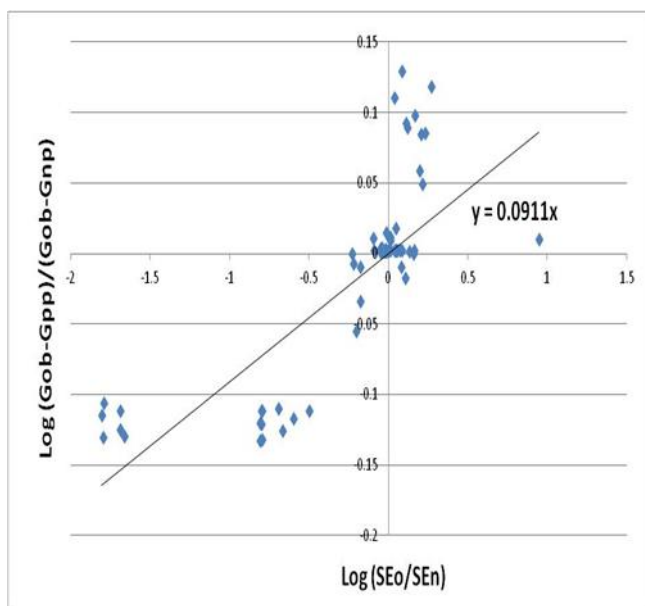


Figure (2). Determination of the exponent (m) in equation (4).

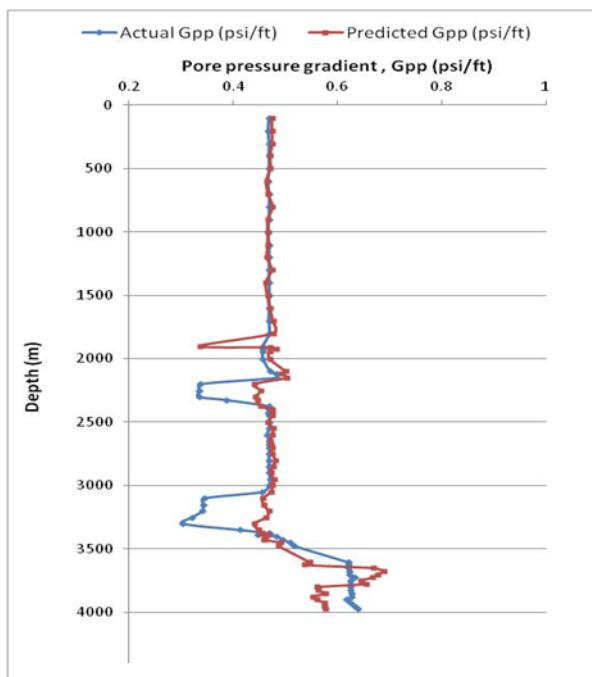


Figure (3) Predicted pore pressure gradient by Rabia approach vs. depth formula compared with the actual pore pressure gradient

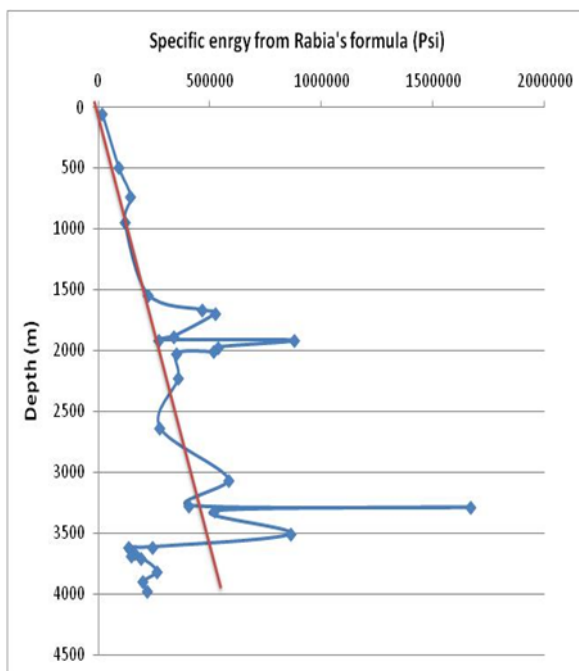


Figure (4) Specific energy obtained by the modified approach of specific energy

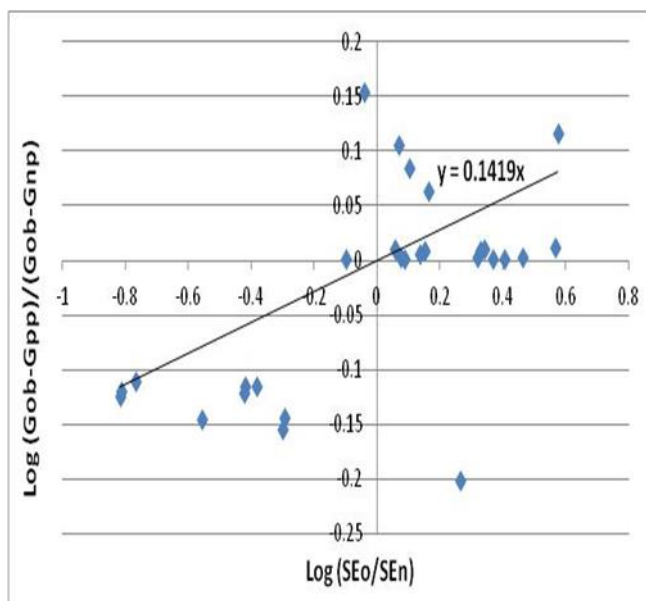


Figure (5) Estimation of the power (m) in equation (4) for Ru-13 formula with the gradient vs. depth

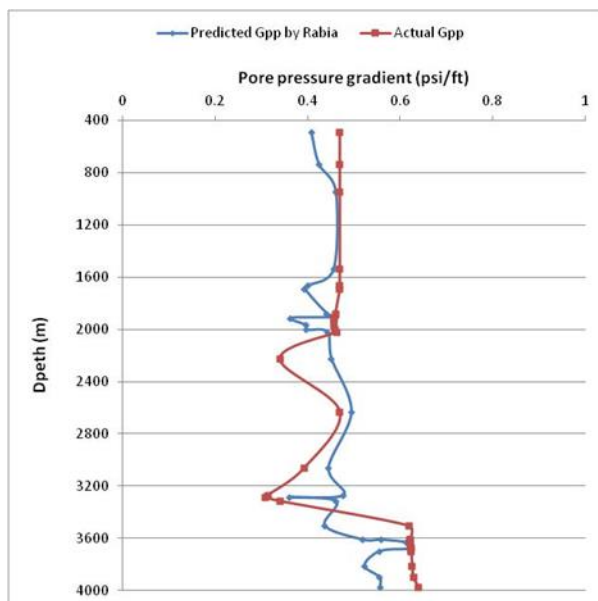


Figure (6) Pore pressure gradient predicted by the new model using Rabia's of specific energy compared actual pore pressure.

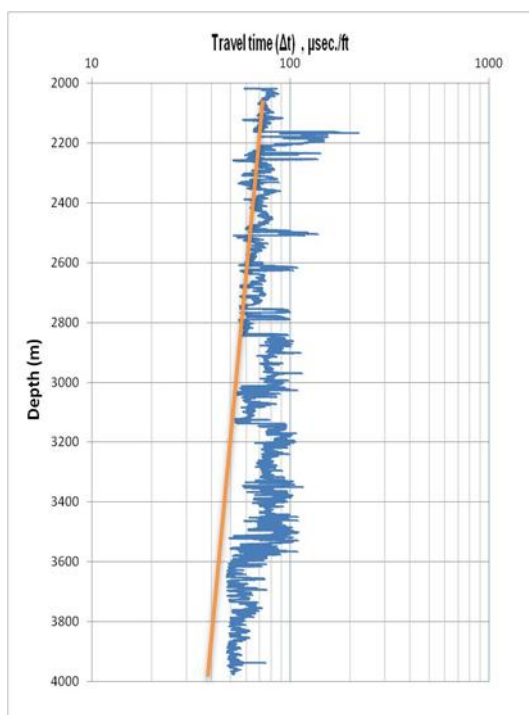


Figure (7) Sonic travel time obtained from showing the normal trend line .

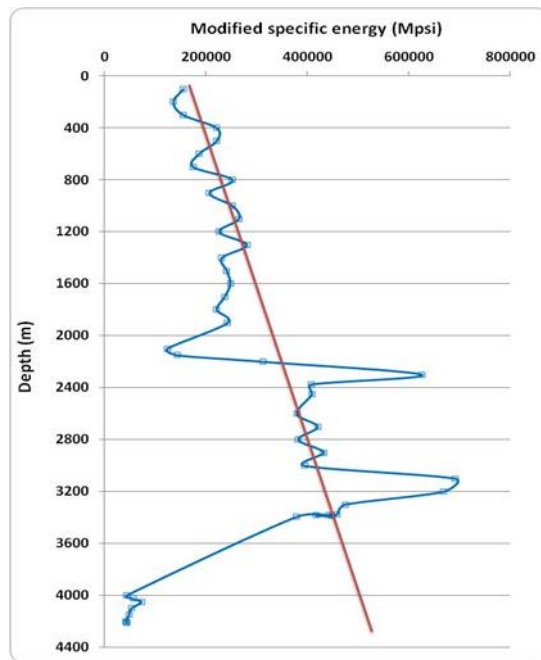


Figure (8) Forecasted pore pressure sonic log gradient from Eaton method vs.

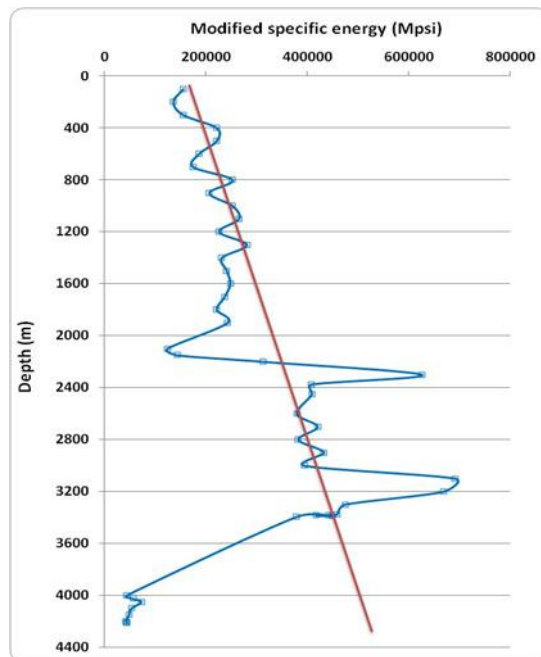


Figure (9) Specific energy from the new formula versus depth for well Zb-42

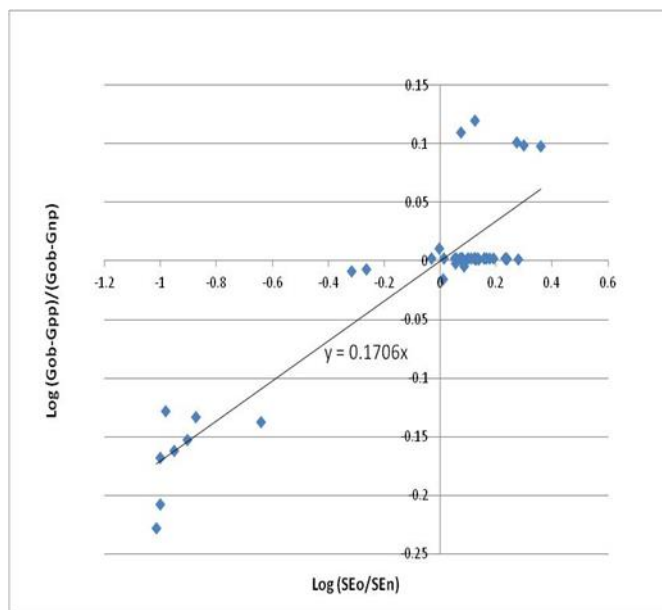


Figure (10) Slope (m) determination from equation (4) for well Zb-42

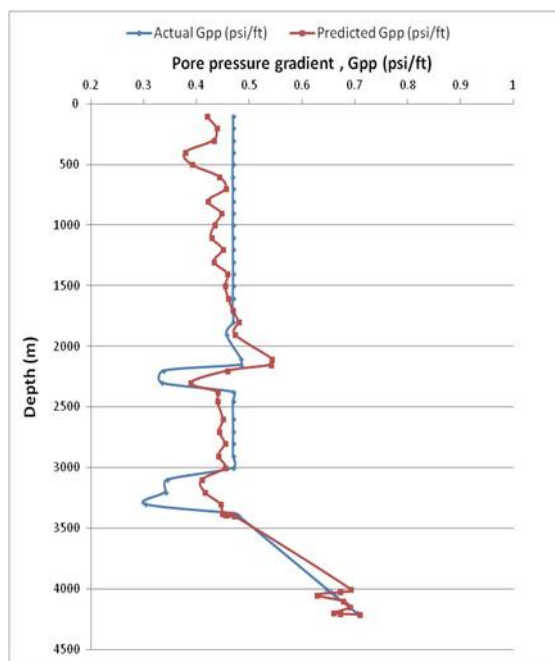


Figure (11) Pore pressure gradient predicted by the new suggested formula along with the actual pressure gradient vs. depth

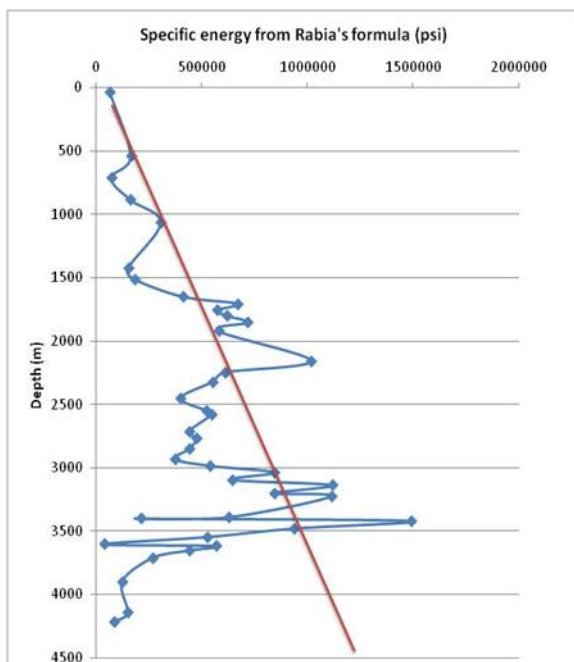


Figure (12) SE obtained from Rabia's method for well Zb-42

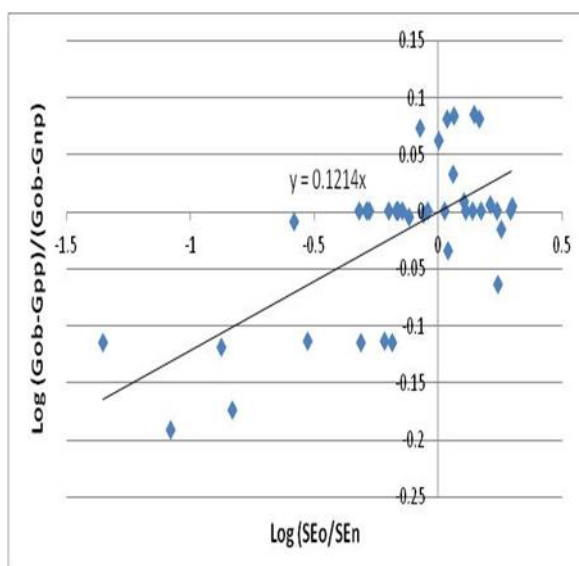


Figure (13) Determination of the exponent (m) from the new model according to Rabia

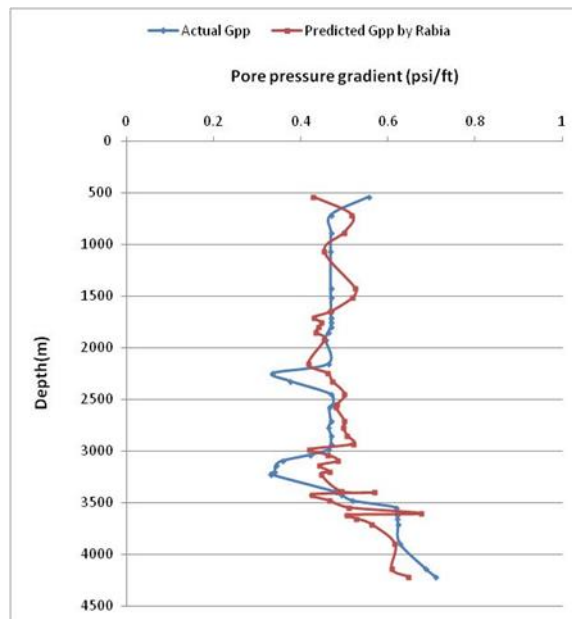


Figure (14) Forecasted formation gradient obtained from equation (4) according to Rabia's formula

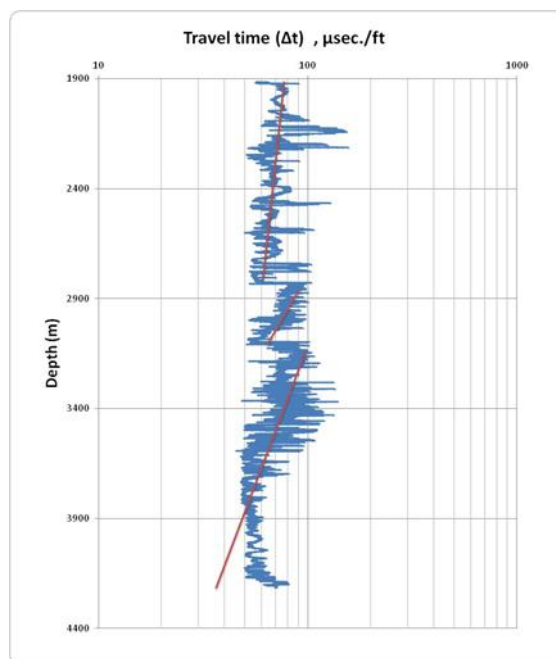


Figure (15) Transit travel time normal From sonic log vs. depth showing the normal compaction trend line

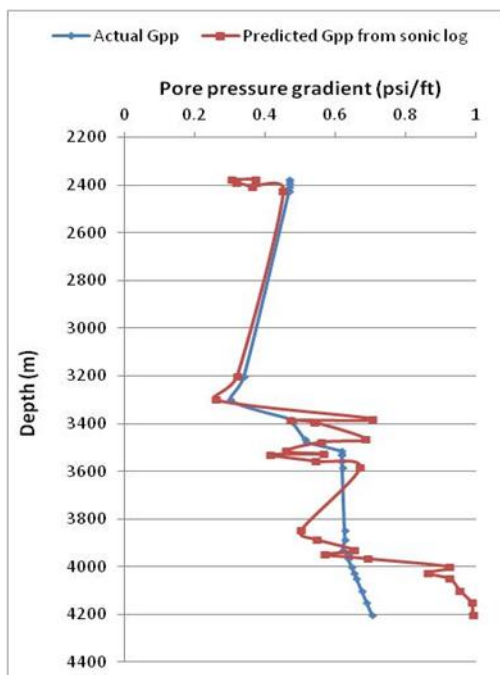


Figure (16) Predicated pore pressure gradient estimated from Eaton's equation along with the actual pore pressure gradient versus depth

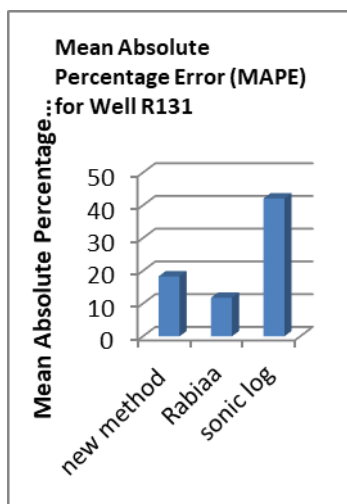


Figure (17). MAPP for131

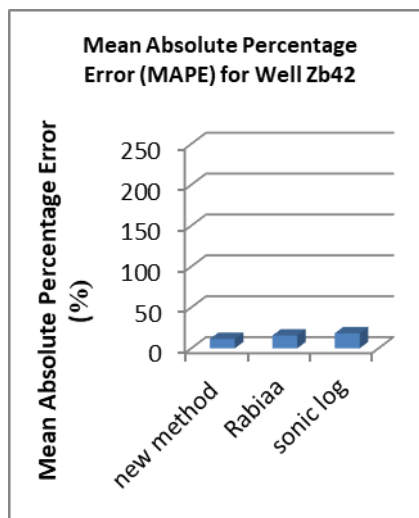


Figure (18). MAPP for Zb42

## Nomenclature

A(I)c	calculated value
A(I)m	measured values( actual value)
APPE	absolute Average percentage error
dcn	dc – exponent from the normal compaction trend at a given depth
dco	computed dc – exponent from the measured data at a given depth
Gnp	normal pore pressure gradient at a given depth (psi/ft)
Gob	overburden pressure gradient at a given depth (psi/ft)
Gpp	pore pressure gradient at a given depth (psi/ft)
Ha	hardness of rock formation
Hw	hardness of bit
MAE	mean absolute error
MES	Mechanical specific energy(psi)
MWD	measurement while drilling
n	number of readings
NTC	normal compaction Trend line
RFT	Repeated Flow test
Rn	normal compaction trend shale resistivity at a given depth(ohm – m)
Ro	observed shale resistivity at a given depth (ohm – m)
ROP	rate of penetration (ft/hr)
SEn	normal Specific energy
SEo	Specific energy observed
T	Torsion or torque (lb-ft)
$\Delta t_n$	normal compaction shale travel time at a given depth (microsecond –ft)
$\Delta t_o$	observed shale travel time at a given depth (micro-second/ft)
Pp	pore pressure

## References

- [1]. Abbas ,K.R, 1996. prediction of abnormal formation pressure in southern Iraq,A master dissertation submmitted to the collage of engineering , pterolume dept. university of Baghdad.
- [2]. Abbas,R,K, 2017. super intendence of Bit Dullnuss Using a New Technique for Nasriya oil wells. journal of Bablyon university /Engineering Sciences, Volume 25, pp. 579-592.
- [3]. Abd Al-Razzaq ,A.,Dabbaj,A.-A.and Hadi,F ., 2016. optimization of Hole cleaning In Iraqi Directional oil wells. Jouneral of Engineering, November , Volume 22, pp. 108-117.
- [4]. Al-Hameedi, A.T., Dunn-Norman, S., Alkinani, H.H., Flori, R.E., and Hilgedick, S.A., 2017. Limiting Drilling Parameters to Control Mud Losses in the Dammam Formation, South Rumaila Field, Iraq. one petero.
- [5]. Almalikee, H.S.A., Al-Najim, F.M.S. ,2018 .Overburden stress and pore pressure prediction for the North Rumaila oilfield, Iraq. Model. Earth Syst. Environ. 4, 1181–1188.
- [6]. Eaton, B.A., 1972. The effect of petroleum overburden stress on Geopressure predication from well logs. Petroleum Technology, August, 24(08), pp. 929-934.
- [7]. Eaton, B.A., 1975. The Equation for Geopressure predications from Well Logs. Society of Petroleum Engineering, 28 September-1October.p. 11.
- [8]. Jincal Zhang, Shangxian Yin, 2017. Real-Time Pore Pressure Detection: Indicators and Improved Methods. Hindawi, p. 12.
- [9]. Cheng Fenga, Zhiwei Wangb, Xili Dengc, Jinhua Fud, Yujiang Shid, Haining Zhange., 2019. A new empirical method based on piecewise linear model to predict static. *Journal of Petroleum Science and Engineering*, April, Volume 175, pp. 1-8.
- [10]. Rabia, H, 1985. Specific Energy as a criterion for Bit selection. journal of Petroleum Technology, July, 37(07), pp. 1225-1229.